

Tunable Double Negative Band Structure from Non-Magnetic Coated Rods

Yue Chen¹ Robert Lipton²

¹ Department of Mathematics Louisiana State University Baton Rouge, LA 70803, USA. email: chenye@math.lsu.edu

² Department of Mathematics, Louisiana State University, Baton Rouge, LA 70803, USA. email: lipton@math.lsu.edu

Abstract

A system of periodic poly-disperse coated nano-rods is considered. Both the coated nano-rods and host material are non-magnetic. The exterior nano-coating has a frequency dependent dielectric constant and the rod has a high dielectric constant. A negative effective magnetic permeability is generated near the Mie resonances of the rods while the coating generates a negative permittivity through a field resonance controlled by the plasma frequency of the coating and the geometry of the crystal. The explicit band structure for the system is calculated in the sub-wavelength limit. Tunable pass bands exhibiting negative group velocity are generated and correspond to simultaneously negative effective dielectric permittivity and magnetic permeability. These can be explicitly controlled by adjusting the distance between rods, the coating thickness, and rod diameters.

Short title: Tunable Double Negative Band Structure
PACS 42,78

1 Introduction

Metamaterials are new class of man made materials that impart unconventional electromagnetic properties derived from sub-wavelength configurations of different conventional materials [1]. The first such materials were seen to exhibit behavior associated with negative bulk dielectric constant [2] and were constructed from a cubic lattice of metal wires. Subsequently negative effective magnetic permeability at microwave frequencies [1] were derived from periodic arrays of non-magnetic metallic split ring resonators [1]. Double negative or left handed metamaterials with simultaneous negative bulk permeability and permittivity at microwave frequencies have been developed using periodic arrays of metallic posts and split ring resonators [3]. Subsequent work has delivered several new designs using different configurations of metallic resonators for double negative behavior [4, 5, 6, 7, 8, 9, 10].

For higher frequencies in the infrared and optical range an alternate strategy for constructing negative effective permeability from non-magnetic components relies on Mie resonances associated with small rods or particles made from high permittivity materials [11]. A double negative metamaterial may be achieved by coating the high permittivity material with a frequency dependent plasmonic or Drude type coating [12] as well as coatings with more general frequency dependence [13].

In this article we focus on the second approach and propose periodic assemblages of aligned non-magnetic dielectric rods each clad with a non-magnetic plasmonic coating. For this case we are able to explicitly calculate the propagation band structure in the sub-wavelength limit. The pass bands and stop bands are given by formulas that depend explicitly on the rod diameters and coating thickness. We show how to construct tunable pass bands associated with double negative effective properties. The physical origin of the negative effective permeability is due to the excitations of Mie resonances inside the rods. On the other hand the negative effective permittivity is caused by

the extreme dielectric properties near the plasma resonance of the coating. We provide the explicit relationship linking Mie resonances and the frequency dependent effective permittivity to the spacing of the rods, the rod radii, and the coating thickness for the coated rod assemblage proposed here.

These relationships are found not by appealing to effective medium theory based on the Clausius-Mossotti formula, but instead we show that it is profitable to take a different approach and characterize wave propagation using explicit multiscale expansions for waves inside the photonic crystal. The wave number associated with a Bloch wave inside the d -periodic crystal is denoted by $k = 2\pi/\lambda$ where λ is the wavelength. The approach taken here provides an explicit power series expansion for the fields in the parameter $\eta = dk$. We outline a systematic framework in which the homogenized dispersion relation is recovered directly from the expansion in the subwavelength $d \ll \lambda$ limit. We introduce photonic crystals made from coated rod assemblages and obtain explicit homogenized dispersion relations for these geometries. The dispersion relations provide explicit conditions on the the distance between neighboring rods, rod radii, and coating thickness necessary for generating pass bands associated with double negative behavior. Two examples are provided showing how the band structure can be manipulated to generate double negative pass bands with negative group velocity.

We conclude referring to related work addressing wave propagation inside high contrast media. When the crystal period and wavelength have the same length scales, the ability to open band gaps for photonic crystals is established and developed in the set of papers [14], [15], and [16]. The power series strategy presented here for subwavelength analysis has been utilized earlier and developed in [17] for characterizing the dynamic dispersion relations for Bloch waves inside plasmonic crystals and for understanding the influence of effective negative permeability on the propagation of Bloch waves inside high contrast dielectrics [18]. Earlier work in two scale homogenization theory for high contrast dielectrics delivers a frequency dependent effective magnetic permeability [19], [20] identical to the generic effective permeability tensor recovered here, see also the work of [21] for homogenization in high contrast media. The connection between high contrast interfaces, homogenization and the associated generation of negative effective magnetic permeability is made in [22]. More recently two-scale homogenization theory has been developed for three dimensional split ring structures that deliver negative effective magnetic permeability [23] and for metal fibers delivering negative effective dielectric constant [24]. A method for creating metamaterials with prescribed effective dielectric permittivity and effective magnetic permeability at a fixed frequency is developed in [25].

2 Electromagnetic fields inside photonic crystals made from coated rods and the subwavelength limit

The meta material is a two-dimensional photonic crystal made of parallel coated rods, see Figure 1. There can be one or more coated rods inside the crystal period. The time harmonic field is p-polarized and the magnetic field inside the crystal is $\mathbf{H} = H(\mathbf{x}) \exp(-i\omega t) \mathbf{e}_3$ where $\mathbf{x} = (x_1, x_2)$ in the x_1x_2 -plane.

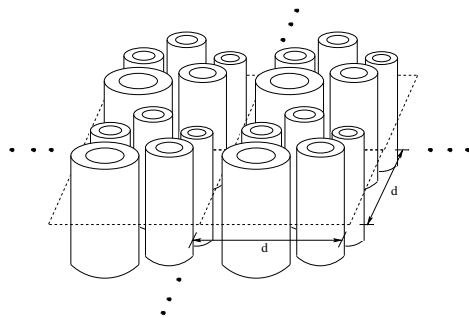


Figure 1: Photonic crystal made from coated rods

The period for the crystal is d and the dielectric coefficient $\epsilon_d(\mathbf{x})$ takes the values

$$\epsilon_d(\mathbf{x}) = \begin{cases} \epsilon_R & \text{in the rod,} \\ \epsilon_p & \text{in the coating,} \\ \epsilon_h & \text{in the host material.} \end{cases} \quad (2.1)$$

The coating is a cylindrical shell of plasmonic material with dielectric constant $\epsilon_p(\omega^2/c^2) = 1 - \frac{\omega_p^2/c^2}{\omega^2/c^2}$. Here ω_p is the plasma frequency associated with the coating material and c is the speed of light in vacuum. The dielectric constant of the rod is chosen according to $\epsilon_R = \frac{\epsilon_r}{d^2}$ where ϵ_r has units of area. The idea is to choose the dielectric permittivity of the rod to be large so that the corresponding Mie resonances are excited in the sub-wavelength limit. The dielectric constant of the host material is given by $\epsilon_h = 1$.

The time harmonic magnetic field for the d -periodic crystal is a Bloch wave

$$H = h(\mathbf{x}) \exp(ik\hat{\kappa} \cdot \mathbf{x}), \quad (2.2)$$

where h is d -periodic in \mathbf{x} , the wave number is given by k , and the direction of propagation in the x_1x_2 -plane is described by the unit vector $\hat{\kappa} = (\hat{\kappa}_1, \hat{\kappa}_2)$. H satisfies the Helmholtz equation

$$\nabla \cdot \epsilon_d^{-1} \nabla H = -\frac{\omega^2}{c^2} H, \quad (2.3)$$

with propagation bands described by dispersion relations involving ω and $k\hat{\kappa}$. We examine the situation in the sub-wavelength limit when d tends to 0. Instead of developing an effective medium theory based on the Clausius-Mossotti formula we show that it is profitable to take a different approach and expand the Bloch wave in a multiscale power series in $\eta = kd$. Here we develop a multiscale power series expansion for h to recover ‘‘homogenized sub-wavelength’’ dispersion relations for plane waves inside a magnetically active double negative effective medium.

We introduce the variable $\mathbf{y} = \mathbf{x}/d$ that takes the period cell of size d into the unit period cell Y . Here Y is split into the subdomains given by the union of rod cross sections R , the rod coatings P and the host H . Figure 2 illustrates a unit cell Y containing one coated rod cross section. The expansion parameter is given by $\eta = kd = \frac{2\pi d}{\lambda}$. The sub-wavelength limit is described by $\eta \rightarrow 0$ for λ fixed. In what follows it is useful to introduce ξ defined by $\xi^2 = \frac{\omega^2}{c^2 k^2}$. The propagation equations satisfied by h for y in the unit period Y are

$$\begin{aligned} -Lh &= \eta^2 \xi^2 h, \text{ in the host,} \\ -Lh &= \eta^2 \xi^2 \epsilon_P(\xi^2 k^2) h, \text{ in the coating,} \\ -Lh &= \epsilon_r \xi^2 k^2 h, \text{ in the rod,} \end{aligned} \quad (2.4)$$

where

$$Lh = \Delta h + 2i\eta\hat{\kappa} \cdot \nabla h - \eta^2 h, \quad (2.5)$$

$$\epsilon_P(\xi^2 k^2) = 1 - \frac{\omega_P^2/c^2}{\xi^2 k^2}, \quad (2.6)$$

and the transmission conditions

$$n \cdot (\nabla h + i\eta\hat{\kappa}h)_{|_H} = n \cdot \epsilon_P^{-1}(\xi^2 k^2) (\nabla h + i\eta\hat{\kappa}h)_{|_C}, \text{ H-C interface,} \quad (2.7)$$

$$n \cdot \epsilon_P^{-1}(\xi^2 k^2) (\nabla h + i\eta\hat{\kappa}h)_{|_C} = n \cdot \left(\frac{\eta^2}{k^2 \epsilon_r} \right) (\nabla h + i\eta\hat{\kappa}h)_{|_R}, \text{ R-C interface.} \quad (2.8)$$

Here the interface separating the host phase and coating phase is denoted by H-C and the interface between the coating phase and the rod is denoted by R-C. Evaluation of quantities on the host side of the interface is denoted by the subscript H , on the coating side by C , and by R on the rod side. The unit normal vector n on the host – coating interface points from the coating into the host and

the unit normal vector on the rod – coating interface points from the rod into the coating. We expand h and ξ^2 as

$$h(d\mathbf{y}) = h_0(\mathbf{y}) + \eta h_1(\mathbf{y}) + \eta^2 h_2(\mathbf{y}) + \dots, \quad (2.9)$$

$$\xi^2 = \xi_0^2 + \eta \xi_1^2 + \eta^2 \xi_2^2 + \dots \quad (2.10)$$

where each term in the expansion is continuous in \mathbf{y} and periodic on Y . Substitution of the expansion into (2.4), (2.7), and (2.8) equating like powers of η gives the following equations used to determine h_0 :

$$-\Delta h_0 = 0, \text{ in the host,} \quad (2.11)$$

$$-\Delta h_0 = 0, \text{ in the coating,} \quad (2.12)$$

$$-\Delta h_0 = \epsilon_r \xi_0^2 k^2 h, \text{ in the rod,} \quad (2.13)$$

and transmission conditions,

$$n \cdot (\nabla h_0)|_H = n \cdot \epsilon_P^{-1}(\xi_0^2 k^2) (\nabla h_0)|_C, \text{ H-C interface,} \quad (2.14)$$

$$n \cdot \epsilon_P^{-1}(\xi_0^2 k^2) (\nabla h_0)|_C = 0, \text{ R-C interface.} \quad (2.15)$$

Noting further that h_0 is continuous across these interfaces we apply (2.11), (2.12), (2.14), and (2.15) to discover that h_0 is a constant function $h_0 = \bar{h}$ outside the rods. From linearity it follows that the h_0 field inside the rod can be written as $h_0 = \bar{h}m(\mathbf{y})$ where

$$-\Delta m = \epsilon_r \xi_0^2 k^2 m, \text{ in the rod,} \quad (2.16)$$

and $m = 1$ on the boundary of the rod. Define the function $g(\mathbf{y})$ to be 1 for \mathbf{y} outside the rod and $g(\mathbf{y})$ to be $m(\mathbf{y})$ for \mathbf{y} inside the rod then $h_0(\mathbf{y})$ is defined up to a multiplicative constant \bar{h} and is given by

$$h_0(\mathbf{y}) = \bar{h}g(\mathbf{y}). \quad (2.17)$$

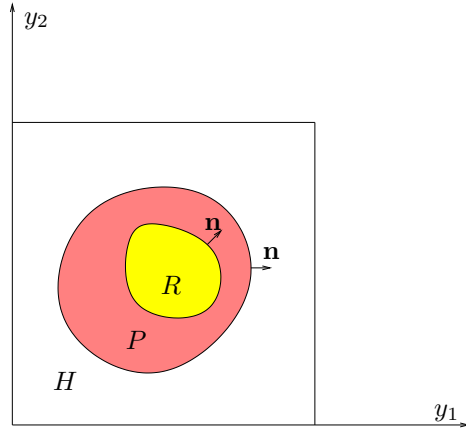


Figure 2: Unit cell containing a single rod cross section. R represents the rod cross section, P the plasmonic coating and H the host.

Next we determine h_1 exterior to the rods. On equating like powers of η we find that

$$-\Delta h_1 = 0, \quad (2.18)$$

outside the rods, and the corresponding transmission conditions for h_1 are given by

$$n \cdot (\nabla h_1 + i\hat{\kappa}\bar{h})|_H = n \cdot \epsilon_P^{-1}(\xi_0^2 k^2) (\nabla h_1 + i\hat{\kappa}\bar{h})|_C, \quad \text{H-C interface}, \quad (2.19)$$

$$n \cdot \epsilon_P^{-1}(\xi_0^2 k^2) (\nabla h_1 + i\hat{\kappa}\bar{h})|_C = 0, \quad \text{R-C interface}. \quad (2.20)$$

The equation (2.18), transmission condition (2.19) and boundary condition (2.20) determine h_1 up to an additive constant c_1 and from the linearity of the problem we write $h_1 = i\bar{h}W \cdot \hat{\kappa} + c_1$. Here $W(\mathbf{y}) = (w_1(\mathbf{y}), w_2(\mathbf{y}))$ where w_i , $i = 1, 2$ are the periodic solutions of the cell problem

$$-\Delta w_i = 0, \quad \text{for } \mathbf{y} \text{ outside the rod}. \quad (2.21)$$

$$n \cdot (\nabla w_i + e^i)|_H = n \cdot \epsilon_P^{-1}(\xi_0^2 k^2) (\nabla w_i + e^i)|_C, \quad \text{H-C interface}, \quad (2.22)$$

$$n \cdot \epsilon_P^{-1}(\xi_0^2 k^2) (\nabla w_i + e^i)|_C = 0, \quad \text{R-C interface}, \quad (2.23)$$

where $e^1 = (1, 0)$ and $e^2 = (0, 1)$. We define the region inside the period cell exterior to the rods by D and introduce the position dependent dielectric constant $\epsilon(\mathbf{y})$ taking the value 1 inside the host and $\epsilon_P(k^2 \xi_0^2)$ inside the coating. For future reference we introduce the tensor $\epsilon_{eff}^{-1}(\xi_0^2 k^2)$ defined by

$$\epsilon_{eff}^{-1}(\xi_0^2 k^2) = \int_D \epsilon(\mathbf{y}) (\nabla W + I) d\mathbf{y}, \quad (2.24)$$

where I is the 2×2 identity tensor.

Now we identify the effective magnetic permeability. Following [1], [11] the average component of the B field parallel to the rods is given by

$$B_{ave} = \frac{1}{d^2} \int_{Y_d} h(\mathbf{x}) e^{i(k\hat{\kappa} \cdot \mathbf{x})} dx_1 dx_2. \quad (2.25)$$

Here Y_d is a period cell for the d -periodic crystal. Substituting the expansion (2.10) for h into (2.25), retaining the lowest order terms and taking $d \rightarrow 0$ gives

$$\lim_{d \rightarrow 0} B_{ave} = \bar{h} \int_Y g(\mathbf{y}) dy_1 dy_2. \quad (2.26)$$

The average component of the H field parallel to the rods is given by [1], [11]

$$H_{ave} = \frac{1}{d} \int_{(0,0,0)}^{(0,0,d)} h(\mathbf{x}) e^{i(k\hat{\kappa} \cdot \mathbf{x})} dx_1 dx_2, \quad (2.27)$$

here the average is taken over any line parallel and exterior to the rods. Sending $d \rightarrow 0$ gives

$$\lim_{d \rightarrow 0} H_{ave} = \bar{h}. \quad (2.28)$$

Using (2.26) and (2.28) the effective permittivity is given by

$$\lim_{d \rightarrow 0} \frac{B_{ave}}{H_{ave}} = \mu_{eff}(\xi_0^2 k^2). \quad (2.29)$$

We recover the explicit form of the effective permeability $\mu_{eff}(\xi_0^2 k^2)$ for a distribution of circular rods inside the unit period cell. To do so recall the following Dirichlet eigenvalues E and eigenfunctions ψ for each rod cross section given by

$$-\Delta \psi = E\psi \quad \text{for } \mathbf{y} \text{ inside rod} \quad \text{and} \quad \psi = 0 \quad \text{for } \mathbf{y} \text{ on rod boundary}. \quad (2.30)$$

For rods with circular cross section of radius $0 < R_r < 1$ and polar coordinates $0 < \rho < R_r$, $0 \leq \theta < 2\pi$, let χ_{nm} be the m th zero of the n th Bessel function, then the Dirichlet eigenvalues are

$E_{nm} = (\chi_{nm}/R_r)^2$, and the corresponding eigenfunctions are $\{J_n(\frac{\chi_{nm}}{R_r}\rho)e^{in\theta}, J_n(\frac{\chi_{nm}}{R_r}\rho)e^{-in\theta}\}$. The associated normalized eigenfunctions are denoted by ψ_{nm}^\pm . Notice that the eigenvalue E_{0m} has only one associated normalized eigenfunction $\psi_{0m} = \frac{J_0(\chi_{0m}(\rho/R_r))}{\sqrt{\pi R} |J_0'(\chi_{0m})|}$ and $\langle \psi_{0m} \rangle^2 = \frac{4\pi R^2}{\chi_{0m}^2}$ when $n = 0$. Here $\langle \cdot \rangle$ denotes the area integral over a rod cross section. It is obvious that $\langle \psi_{nm}^\pm \rangle^2 = 0$ for $n \neq 0$.

Expanding $m(\mathbf{y})$ in the basis ψ_{nm}^\pm noting that $m - 1 = 0$ outside the rods gives for each rod

$$m = 1 - \sum_{m=0}^{\infty} \frac{\xi_0^2 k^2}{\xi_0^2 k^2 - \frac{E_{0m}}{\epsilon_r}} \langle \psi_{0m} \rangle \psi_{0m}. \quad (2.31)$$

For a distribution of rods with radii R_{rj} , $j = 1, \dots, \ell$, we have

$$\mu_{eff}(\xi_0^2 k^2) = \int_Y g(\mathbf{y}) d\mathbf{y} = 1 - \sum_{j=0}^{\ell} N(R_{rj}) \sum_{m=0}^{\infty} \frac{4\pi R_{rj}^2}{\chi_{0m}^2} \frac{\xi_0^2 k^2}{\xi_0^2 k^2 - k_{jm}^2}, \quad (2.32)$$

where $N(R_{rj})$ is the number of rods with radius R_{rj} and $k_{jm}^2 = \frac{\chi_{0m}^2}{\epsilon_r R_{rj}^2}$.

Last we find the homogenized sub-wavelength dispersion relation. Recall that $\xi^2 k^2 = \frac{\omega^2}{c^2}$ and from (2.10)

$$\frac{\omega^2}{c^2} = \frac{\omega_0^2}{c^2} + \eta \frac{\omega_1^2}{c^2} + \eta^2 \frac{\omega_2^2}{c^2} + \dots, \quad (2.33)$$

where

$$\frac{\omega_i^2}{c^2} = \xi_i^2 k^2, \text{ for } i = 0, 1, \dots \quad (2.34)$$

The sub-wavelength dispersion relation identified as the dispersion relation between ω_0 and $k\hat{\kappa}$ given by $\frac{\omega_0^2}{c^2} = \xi_0^2 k^2$. We now recover this dispersion relation by deriving the formula for ξ_0^2 . Equating like powers of η gives the following equations for h_2 exterior to the rods.

$$-(\Delta h_2 + 2i\eta\hat{\kappa} \cdot \nabla h_1 - \eta^2 \bar{h}) = \xi_0^2 \bar{h}, \text{ in the host,} \quad (2.35)$$

$$-(\Delta h_2 + 2i\eta\hat{\kappa} \cdot \nabla h_1 - \eta^2 \bar{h}) = \xi_0^2 \epsilon_P (\xi_0^2 k^2) \bar{h}, \text{ in the coating,} \quad (2.36)$$

and the transmission conditions

$$\begin{aligned} & \left(\xi_0^2 k^2 - \frac{\omega_p^2}{c^2} \right) n \cdot (\nabla h_2 + i\hat{\kappa} h_1)_{|_H} + (\xi_1^2 k^2) n \cdot (\nabla h_1 + i\hat{\kappa} \bar{h})_{|_H} \\ &= (\xi_0^2 k^2) n \cdot (\nabla h_2 + i\hat{\kappa} h_1)_{|_C} + (\xi_1^2 k^2) n \cdot (\nabla h_1 + i\hat{\kappa} \bar{h})_{|_C}, \text{ H-C interface,} \end{aligned} \quad (2.37)$$

$$\begin{aligned} & (\xi_0^2 k^2) n \cdot (\nabla h_2 + i\hat{\kappa} h_1)_{|_C} + (\xi_1^2 k^2) n \cdot (\nabla h_1 + i\hat{\kappa} \bar{h})_{|_C} + (\xi_2^2 k^2) n \cdot \nabla h_0_{|_C} \\ &= \frac{1}{k^2 \epsilon_r} \left(\xi_0^2 k^2 - \frac{\omega_p^2}{c^2} \right) n \cdot \nabla h_0_{|_R}, \text{ R-C interface.} \end{aligned} \quad (2.38)$$

Integrating and adding (2.35) and (2.36) gives the solvability condition

$$\begin{aligned} \xi_0^2 \int_D \bar{h} d\mathbf{y} &= - \int_H (\Delta h_2 + 2i\hat{\kappa} \cdot \nabla h_1 - \bar{h}) d\mathbf{y} \\ &\quad - \int_P \epsilon^{-1} (\xi_0^2 k^2) (\Delta h_2 + 2i\hat{\kappa} \cdot \nabla h_1 - \bar{h}) d\mathbf{y}. \end{aligned} \quad (2.39)$$

On integrating by parts and applying (2.13) together with the transmission conditions (2.15), (2.19), (2.20), (2.37), and (2.38) shows that (2.39) is equivalent to

$$\xi_0^2 = \mu_{eff}^{-1} (\xi_0^2 k^2) \epsilon_{eff}^{-1} (\xi_0^2 k^2) \hat{\kappa} \cdot \hat{\kappa}. \quad (2.40)$$

Writing $\omega_0^2/c^2 = \xi_0^2 k^2$ and substitution into (2.40) delivers the homogenized subwavelength dispersion relation

$$\frac{\omega_0^2}{c^2} = n_{eff}^{-2} k^2, \quad (2.41)$$

where the effective index of diffraction n_{eff}^2 is given by

$$n_{eff}^2 = \mu_{eff} \left(\frac{\omega_0^2}{c^2} \right) \left(\epsilon_{eff}^{-1} \left(\frac{\omega_0^2}{c^2} \right) \hat{\mathbf{k}} \cdot \hat{\mathbf{k}} \right)^{-1}. \quad (2.42)$$

Applying (2.9) and collecting results shows that to lowest order the Bloch waves $H = h(\mathbf{x})e^{i(k\hat{\mathbf{k}} \cdot \mathbf{x} - t\omega)}$ inside the photonic crystal are given by the subwavelength expansion

$$H(\mathbf{x}, t) = \left(\bar{h}g\left(\frac{\mathbf{x}}{d}\right) + \eta h_1\left(\frac{\mathbf{x}}{d}\right) + O(\eta^2) \right) \exp i(k\hat{\mathbf{k}} \cdot \mathbf{x} - t(\omega_0 + \eta\omega_1 + O(\eta^2))). \quad (2.43)$$

In the subwavelength limit the spatial averages of H correspond to spatial averages of plane waves associated with a magnetically active effective medium. To see this take any planar averaging domain S and pass to the $d \rightarrow 0$ limit in the average to get

$$\begin{aligned} \lim_{d \rightarrow 0} \frac{1}{Area(S)} \int_S H(\mathbf{x}, t) dx_1 dx_2 &= \lim_{d \rightarrow 0} \frac{1}{Area(S)} \int_S \bar{h}g\left(\frac{\mathbf{x}}{d}\right) \exp i(k\hat{\mathbf{k}} \cdot \mathbf{x} - t\omega_0) dx_1 dx_2 \\ &= \frac{1}{Area(S)} \int_S \mu_{eff} \bar{h} \exp i(k\hat{\mathbf{k}} \cdot \mathbf{x} - t\omega_0) dx_1 dx_2. \end{aligned} \quad (2.44)$$

In a similar way, taking averages over any interval $a < x_3 < b$ on any line parallel to the x_3 axis not intersecting the coated rods gives

$$\begin{aligned} \lim_{d \rightarrow 0} \frac{1}{b-a} \int_{(0,0,a)}^{(0,0,b)} H(\mathbf{x}, t) dx_3 &= \lim_{d \rightarrow 0} \frac{1}{b-a} \int_{(0,0,a)}^{(0,0,b)} \bar{h}g\left(\frac{\mathbf{x}}{d}\right) \exp i(k\hat{\mathbf{k}} \cdot \mathbf{x} - t\omega_0) dx_3 \\ &= \frac{1}{b-a} \int_{(0,0,a)}^{(0,0,b)} \bar{h} \exp i(k\hat{\mathbf{k}} \cdot \mathbf{x} - t\omega_0) dx_3. \end{aligned} \quad (2.45)$$

Thus the appropriate averages of the plane waves $H_{hom} = \bar{h} \exp i(k\hat{\mathbf{k}} \cdot \mathbf{x} - t\omega_0)$ and $B_{hom} = \mu_{eff} \bar{h} \exp i(k\hat{\mathbf{k}} \cdot \mathbf{x} - t\omega_0)$ provide approximations to the average field seen in the d periodic photonic crystal for $0 < d \ll k$.

3 Electromagnetic fields inside coated rod assemblages

Here we introduce a special class of photonic crystals made from coated rod assemblages and derive an explicit formula for the subwavelength dispersion relation (2.41). The formula shows how the band structure depends explicitly on the distribution of rod radii, coating thickness and distance between neighboring rods. The assemblage is described as follows. Consider first the unit period cell Y filled with disks with radii ranging down to the infinitesimal. Inside each disk we place a centered rod cross section then a concentric coating of plasmonic material and finally a concentric coating of host material, see Figure 3.

The cross sections of the coated rods together with the connected host material is depicted in Figure 4. The ratio of the radii of the rod cross section, plasmonic coating, and host coating are the same for all the disks and we denote the area fractions of the host, coating, and core phases by θ_H , θ_P , and θ_R respectively, see Figure 3. The radii of the rods used in the assemblage is denoted by $R_{r1} > R_{r2} > R_{r3} \dots$. The number of rods having radius R_{rj} are denoted by $N(R_{rj})$. For rods of radii R_{rj} the outer radii of the core is denoted by R_{pj} and the distance to the nearest neighboring rod is R_{hj} . for the coated rod assemblage it is clear that R_{hj} is determined by R_{rj} together with θ_R and θ_P .

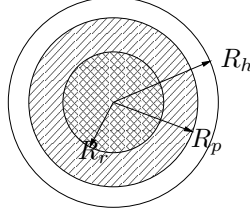


Figure 3: Doubly Coated Cylinder

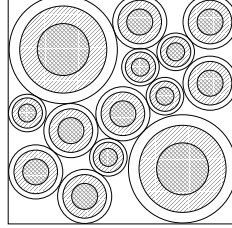


Figure 4: Cross section of the unit period filled with coated rods. The coated rods fill all space.

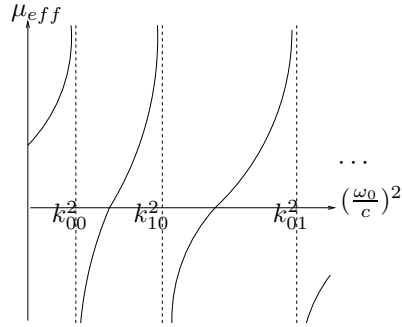


Figure 5: the relation between μ_{eff} and $(\omega_0/c)^2$

This type of configuration is known in the composites literature and is referred to as a doubly coated cylinder assemblage [26], [27], [28], [29]. The explicit formula for μ_{eff} follows from (2.32) and is given by

$$\mu_{eff} \left(\frac{\omega_0^2}{c^2} \right) = 1 - \sum_{j=0}^{\infty} N(R_{rj}) \sum_{m=0}^{\infty} \frac{4\pi R_{rj}^2}{\chi_{0m}^2} \frac{(\omega_0/c)^2}{(\omega_0/c)^2 - k_{jm}^2}. \quad (3.1)$$

The poles of $\mu_{eff}(\omega_0^2/c^2)$ are given by k_{jm}^2 , see Figure 5.

The explicit formula for the effective dielectric permittivity follows from a standard calculation using (2.21), (2.21), (2.22) and (2.23) (see, for example [30]) and is given by

$$\epsilon_{eff}^{-1} = \epsilon_H^{-1} + \frac{2(1 - \theta_H)\epsilon_H^{-1}}{\theta_H - \frac{2\epsilon_H^{-1}}{\epsilon_H^{-1} - \epsilon_C^{-1}}} \quad (3.2)$$

with

$$\epsilon_C^{-1} = \epsilon_P^{-1} + \frac{2\theta_R\epsilon_P^{-1}}{2\theta_R - \theta_P}. \quad (3.3)$$

On writing $\epsilon_p(\omega_0^2/c^2) = 1 - \frac{\omega_p^2/c^2}{\omega_0^2/c^2}$ and $\epsilon_H = 1$ we obtain the formula for the frequency dependent effective dielectric tensor given by

$$\epsilon_{eff} \left(\frac{\omega_0^2}{c^2} \right) = \frac{1 - (\theta_R + \theta_P)}{1 + \theta_R + \theta_P} \left(\frac{\frac{1 + \theta_R + \theta_P}{1 - (\theta_R + \theta_P)} + \left(1 - \frac{(\omega_p/c)^2}{(\omega_0/c)^2} \right)^{-1} \left(\frac{\theta_P}{2\theta_R + \theta_P} \right)}{\frac{1 - (\theta_R + \theta_P)}{1 + \theta_R + \theta_P} + \left(1 - \frac{(\omega_p/c)^2}{(\omega_0/c)^2} \right)^{-1} \left(\frac{\theta_P}{2\theta_R + \theta_P} \right)} \right). \quad (3.4)$$

The dependence of μ_{eff} and ϵ_{eff} on the rod diameter and coating thickness and host area fraction is explicitly given by (3.1) and (3.4). This explicit dependence allows for the tuning of the dispersion relation

$$k^2 = \frac{\omega_0^2}{c^2} n_{eff}^2, \quad (3.5)$$

where

$$n_{eff}^2 = \mu_{eff} \left(\frac{\omega_0^2}{c^2} \right) \epsilon_{eff} \left(\frac{\omega_0^2}{c^2} \right). \quad (3.6)$$

For each coated rod with radius R_{rj} , outer coating radius R_{pj} and nearest neighbor distance R_{hj} the h_0 field inside the rod is given by (2.31) and the h_1 field outside the rod is

$$h_1 = (1 + \theta_R)^{-1} \left(r \cos \gamma + \frac{R_{rj}^2}{r} \cos \gamma \right), \quad R_{rj} < r < R_{pj}, \quad (3.7)$$

$$h_1 = \frac{2\theta_R + \theta_P + \theta_P \left(1 - \frac{\omega_p^2/c^2}{\omega_0^2/c^2} \right)^{-1}}{F} r \cos \gamma + \frac{2\theta_R + \theta_P - \theta_P \left(1 - \frac{\omega_p^2/c^2}{\omega_0^2/c^2} \right)^{-1}}{F} \frac{R_{pj}^2}{r} \cos \gamma, \quad R_{pj} < r < R_{hj}, \quad (3.8)$$

where (r, γ) are local polar coordinates inside the coated rod and F is given by

$$F = (2\theta_R + \theta_P)(1 + \theta_R + \theta_P) + \left(1 - \frac{\omega_p^2/c^2}{\omega_0^2/c^2} \right)^{-1} \theta_P(1 - (\theta_R + \theta_P)). \quad (3.9)$$

It is clear that h_0 diverges inside the rods with radii R_{rj} as ω_0^2/c^2 approaches k_{jm}^2 while h_1 diverges in the neighborhoods of all the coated rods, $R_{pj} < r < R_{hj}$ as ω_0^2/c^2 approaches the zero of $\epsilon_{eff} \left(\frac{\omega_0^2}{c^2} \right)$.

4 Tunable double negative behavior

When ϵ_{eff} and μ_{eff} have the same sign it is clear that $n_{eff}^2 > 0$ and wave propagation occurs. In this section, we show that it is possible to tune the assemblage through the choice of rod radii, coating thickness and host volume fraction to exhibit single negative, double negative, and double positive behavior depending on the signs of ϵ_{eff} and μ_{eff} . For coated cylinder assemblages it is evident that the distance between neighboring rods and the coating thickness is explicitly determined by the area fraction of the host phase, the area fraction of the rods and the rod radii R_{rj} . The dielectric function (3.4) has only one pole and one zero and these depend explicitly on the geometry of the coated rod assemblage and are given by

$$p = \left(\frac{\omega_p}{c} \right)^2 \frac{\theta_H(2\theta_R + \theta_P)}{\theta_H(2\theta_R + \theta_P) + (2 - \theta_H)\theta_P} \quad (4.1)$$

and

$$p^* = \left(\frac{\omega_p}{c} \right)^2 \frac{(2 - \theta_H)(2\theta_R + \theta_P)}{(2 - \theta_H)(2\theta_R + \theta_P) + \theta_H\theta_P}. \quad (4.2)$$

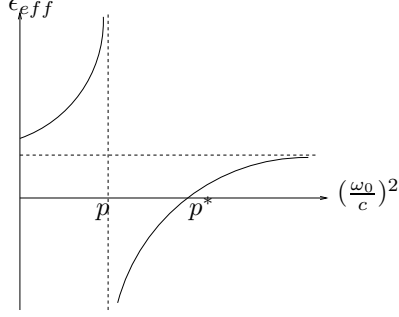


Figure 6: the relation between ϵ_{eff} and $(\omega_0/c)^2$

Observe that $p < p^*$ and ϵ_{eff} is negative when $p < (\omega_0/c)^2 < p^*$. The relation between ϵ_{eff} and $(\omega_0/c)^2$ is displayed in Figure 6.

From Figure 5 and Figure 6, it is clear that both ϵ_{eff} and μ_{eff} are negative for $p < (\omega_0/c)^2 < p^*$ provided that $(\omega_0/c)^2$ is simultaneously greater than but close to the poles of μ_{eff} . Therefore for ϵ_{eff} and μ_{eff} to be simultaneously negative it is required that $p < k_{jm}^2 < p^*$, i.e., the assemblage must contain rods with radii R_{rj} satisfying the condition

$$\frac{\chi_{0m}^2 c^2 (2 - \theta_h)(2\theta_r + \theta_p) + \theta_h \theta_p}{\epsilon_r \omega_p^2 (2 - \theta_h)(2\theta_r + \theta_p)} < R_{rj}^2 < \frac{\chi_{0m}^2 c^2 \theta_h (2\theta_r + \theta_p) + (2 - \theta_h)\theta_p}{\epsilon_r \omega_p^2 \theta_h (2\theta_r + \theta_p)}. \quad (4.3)$$

Now we fix the area fractions $\theta_R = 0.8, \theta_P = 0.1, \theta_H = 0.1$, and set $\omega_p = 25.8$ THz and $\epsilon_r = 200m^2$ so that $p = 0.349 \times 10^{10} m^{-2}$ and $p^* = 0.737 \times 10^{10} m^{-2}$. The dispersion relation $k^2 = (\frac{\omega}{c})^2 n_{eff}^2$ is displayed in Figure 7 for an assemblage with the two largest rod radii chosen to be $R_{r0} = 0.2$ and $R_{r1} = 0.17$. These radii satisfy the requirement given by (4.3) while the radii of all other rods in the assemblage are chosen to lie below these two values and do not satisfy (4.3). It is clear from the figure that, $\epsilon_{eff} < 0$ when $p < (\omega_0/c)^2 < p^*$ and otherwise $\epsilon_{eff} \geq 0$. In this example, p is below k_{00}^2 and p^* lies between k_{00}^2 and k_{10}^2 . Notice in Figure 7 that the slope is negative for the dispersion curve lying between k_{00}^2 and p^* , indicating a negative group velocity.

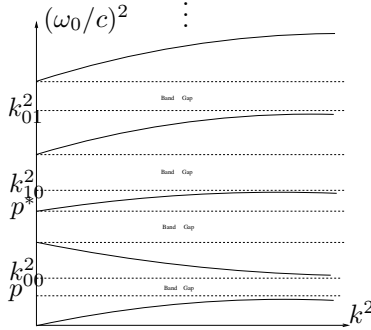


Figure 7: Dispersion relation $k^2 = (\frac{\omega_0}{c})^2 n_{eff}^2$ for a material with $\epsilon_p = 1 - \frac{\omega_p^2/c^2}{\omega_0^2/c^2}$ where $\omega_p = 25.8$ THz. The assemblage contains rods of radii $R_{r0} = 0.2$ and $R_{r1} = 0.17$.

In Figure 8, we choose the largest two radii to be given by $R_{r0} = 0.2$ and $R_{r1} = 0.18$ and all other rods have radii below these values. For this case, p is below k_{00}^2 but p^* is between k_{10}^2 and k_{01}^2 .

Notice that for points \mathbf{x} inside the coating phase and for $(\omega_0/c)^2$ close to k_{0m}^2 , that (2.31) and

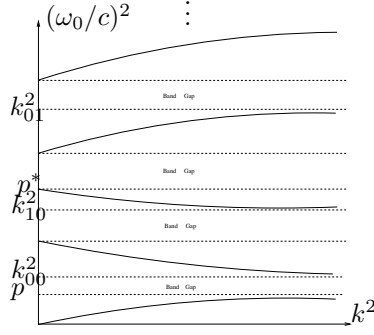
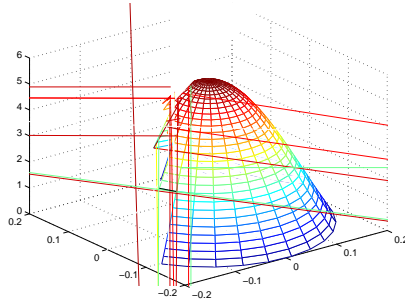


Figure 8: Dispersion relation $k^2 = (\frac{\omega_0}{c})^2 n_{eff}^2$ for a material with $\epsilon_p = 1 - \frac{\omega_p^2/c^2}{\omega_0^2/c^2}$ where $\omega_p = 25.8$ THz. The largest two rod radii appearing in the assemblage are given by $R_{r0} = 0.2$ and $R_{r1} = 0.18$.

(2.43) show that $H(\mathbf{x}, t)$ behaves like $h(\mathbf{x})e^{i(k\hat{\mathbf{k}}\cdot\mathbf{x}-t\omega)}$ where

$$h(\mathbf{x}) = \mu_{eff}^{-1} \bar{h} e^{ik\hat{\mathbf{k}}\cdot\mathbf{x}} \left(1 - \frac{(\omega_0/c)^2}{(\omega_0/c)^2 - k_{0m}^2} \langle 1 | \psi_{0m} \rangle \right) \psi_{0m}. \quad (4.4)$$

In particular, when $(\omega_0/c)^2$ is near k_{00}^2 , the profile of h is ψ_{00} (see Figure 9 with $R_{r0} = 0.2$) and when $(\omega_0/c)^2$ is near k_{01}^2 , the profile of h is ψ_{01} (see Figure 10 with $R_{r0} = 0.2$).



5 Acknowledgements

This research is supported by NSF grant DMS-0807265 and AFOSR grant FA9550-05-0008.

References

- [1] Pendry, J., Holden, A., Robbins, D. and Stewart, W. 1999 *IEEE Trans. Microwave Theory Tech.* 47(11) 2075-2084.
- [2] Pendry, J., Holden, A., Robbins, D. & Stewart, W. 1998 *J. Phys.: Condens. Matter.* 10 4785-4809.
- [3] Smith, D., Padilla, W., Vier, D., Nemat-Nasser, S. & Schultz, S. 2000 *Phys. Rev. Lett.* 84(18) 4184-4187.
- [4] Huangfu, J., Ran, L., Chen, H., Zhang, X., Chen, K., Grzegorzczuk, T. M., & Kong, J., A. 2004 *Appl. Phys. Lett.* 84 1537.
- [5] Zhang, F. L., Potet, S., Carbonell, J., Lheurette, E., Vanbesien, O., Xiaopeng, Z., & Lippens, D. 2008 *IEEE Trans. Microw. Theory Tech.* 56 2566.
- [6] Enkrich, C., Wegener, M., Linden, S., Burger, S., Zschiedrich, L., Schmidt, F., Zhou, J.F., Koschny, T., & Soukoulis, C. M. 2005 *Phys. Rev. Lett.* 95 203901.
- [7] Zhang, S., Fan, W., Minhas, B. K., Frauenglass, A., Malloy, K. J., & Brueck, S. R. J. 2005 *Phys. Rev. Lett.* 94 037402.
- [8] Shalaev, V. M., Cai, W., Chettiar, U. K., Yuan, H. K., Sarychev, A. K., Drachev, V. P., & Kildishev, A. V. 2005 *Opt. Lett.* 30(24) 3356-3358.
- [9] Zhou, X., and Zhao, X. P. 2007 *Appl. Phys. Lett.* 91 181908.
- [10] Dolling, G., Enrich, C., Wegener, M., Soukoulis, C. M., & Linden, S. 2006 *Opt. Lett.* 31 1800-1802.
- [11] O'Brien, S., and Pendry, J. B. 2002 *J. Phys.: Condens. Matter* 14 4035-4044.
- [12] Wheeler, M. S., Aitchison, J. S., & Mojahedi, M. 2005 *Phys. Rev. B* 73 045105.
- [13] Yannopoulos, V., 2007 *Phys. Stat. Sol. (RRL)* 1(5) 208210.
- [14] Figotin, A. and Kuchment, P., 1996 *SIAM Journal on Applied Mathematics* 56(1) 68-88.
- [15] Figotin, A. and Kuchment, P., 1996 *SIAM Journal on Applied Mathematics* 56(6) 1561-1620.
- [16] Figotin, A. and Kuchment, P., 1998 *SIAM Journal on Applied Mathematics* 58(2) 683-702.
- [17] Fortes, S. P., Lipton, R. P., Shipman, S. P. 2010 *Proc. R. Soc. Lond. Ser. A* doi: 10.1098/rspa.2009.0542.
- [18] Fortes, S. P., Lipton, R. P., Shipman, S. P. 2010 Preprint.
- [19] Bouchitté, G. & Felbacq, D. 2005 *New Journal of Physics* 7 159.
- [20] Bouchitté, G. & Felbacq, D. 2004 *C. R. Acad. Sci. Paris* I(339) 377-382.
- [21] Zhikov, V., V., 2004 *Algebra i Analiz* 16 3458, English translation in 2005 *St. Petersburg Mathematical Journal* 16 (5) 773790.
- [22] Kohn, R. & Shipman, S. 2008 *SIAM Multiscale Model Simul.* 7(1) 62-92.
- [23] Bouchitté, G. & Schweizer, B. 2010 *SIAM Journal on Multiscale Modeling and Simulation*, To appear.

- [24] Bouchitté G. & Bourel, C. 2010 *Communications in Computational Physics*, To appear.
- [25] Milton, G., W. 2010 *New Journal of Physics* 12(3) 033035.
- [26] Schulgasser, K. 1997 *International Journal of Heat and Mass Transfer* 20 1226–1230.
- [27] Milton, G., W. 1981 *Applied Physics* A26 125–130.
- [28] Lurie, K., A. & Cherkaev, A., V., 1985 *Journal of Optimization Theory and Applications* 46 571–589.
- [29] Milgrom, M. 1989 *Journal of Applied Physics* 66 3429–3436.
- [30] Milton, G.W. 2002 *The Theory of Composites*. Cambridge University Press, Cambridge.